DOI: 10.1478/AAPP.1031A2

AAPP | Atti della Accademia Peloritana dei Pericolanti
Classe di Scienze Fisiche, Matematiche e Naturali
ISSN 1825-1242

Vol. 103, No. 1, A2 (2025)

CUSTOMIZATION OF LIMITED AREA MODEL FOR COMPLEX OROGRAPHY TERRITORIES: THE WRF AND THE WRF-CHEM UNIME MODEL

MARIA TERESA CACCAMO [a], ALESSANDRO BONCALDO [ab], LORENZO PISTORINO [a], AGOSTINO SEMPREBELLO [b] AND SALVATORE MAGAZÙ [ab] *

ABSTRACT. Since ancient times, knowledge of weather conditions has been essential for human survival and for planning activities. In this context, atmospheric forecast models play a key role in weather studies, contributing significantly to understand and predict short- and long-term weather changes. In the field of atmospheric modelling, weather forecast models can be classified into Global Models (GMs) and Limited Area Models (LAMs) in relation to their both domain coverage and spatial resolution. Especially in the last few years, the application of LAMs with high spatial resolution has become more and more important, as they can perform high-efficiency predictions for the increasingly frequent severe weather phenomena. In particular, the Weather Research and Forecasting (WRF) model operates in the field of Numerical Weather Prediction (NWP); it was developed as a result of a collaboration between National Center for Atmospheric Research (NCAR), National Center for Environmental Prediction (NCEP) and Earth System Research Laboratory (ESRL). Furthermore, the WRF-Chem model, which can be considered as the chemical extension of the WRF model, is widely employed for modelling atmospheric pollutants. In this framework, the present contribution is focused, at first, on the optimization steps performed on the WRF model applied to Sicily, a region characterized by a complex orography and peculiar geophysical conditions. In addition, due to the presence of different active volcanoes in Sicily, the WRF-Chem model is also used for forecasting volcanic ash as well as desert dust intrusion. Furthermore, the hardware and software structures of the customized WRF and WRF-Chem models developed at Messina University and the adopted management procedures will be described. In particular, the software routines to follow for the forecast chain and the procedures to be adopted in case of faults will be described step by step. Finally, in order to show the prediction capability of the customized WRF and WRF-Chem models, two case studies will be presented and discussed.

1. Introduction

NWP models play a key role in our understanding of weather phenomena, but it's crucial to remember that like as scientific tools, they can be misused. A mistake that can occur in the use of NWP models is due to the interpretation of results obtained only by pre-compiled models without a critical analysis of the underlying involved physical problems. It is

well known that the models based on NWP are powerful tools but not foolproof. For this reason, it is important to use them with caution, recognizing their limitations and integrating forecast information with local experience and other sources of meteorological data (Scotton *et al.* 2003; Lynch 2007). NWP methods are based on the numerical solution of balance equations that govern atmospheric dynamics (Holton 2004; John M. Wallace 2006; Pielke Sr 2013). To solve these equations, it is necessary to provide the model, as input data, the so-called prognostic variables that include: atmospheric pressure at the ground, horizontal components of wind speed, humidity and air density. As output, the model furnishes the associated variables that are called diagnostic variables, such as: cloud cover, visibility, rainfall quantities and temperature that is evaluated on a finer scale. The equations involved, called primitives, are the following:

- Continuity equation:
$$\frac{d\rho}{dt} = -\rho\nabla\cdot v + S_n \tag{1}$$
where S_n describes the presence of "source" and "sink" terms, ρ is the density and v the velocity.
- The principle of momentum conservation that takes into account the Coriolis force due to the rotational motion of the planet:
$$\frac{dv}{dt} = -\frac{1}{\rho}\nabla p - 2\Omega\wedge v + g \tag{2}$$
where the term $2\Omega\wedge v$ refers to the Coriolis force, p is the pressure and g is the gravitational acceleration.
- The principle of energy balance that corresponds to the first law of Thermodynamics:
$$\frac{de}{dt} = j_Q - p\frac{d\alpha}{dt} \tag{3}$$
where e represents the fraction of energy with respect to the unit of mass, j_Q is the heat flow entering the unit of mass.
- Ideal gas law:
$$pV = nRT \tag{4}$$
where R is the universal gas constant and T is the temperature.
- The law of water balance:
$$\frac{dq}{dt} = S_n \tag{5}$$
where q is the specific humidity.

However, there are no analytic solutions for the primitive equations that are valid for all points in the atmosphere. For this reason, the calculation procedure is facilitated by transforming the atmospheric portion of interest into a three-dimensional grid identified by the grid points. This procedure is known as discretization, and it consists of substituting the derivatives that appear in the primitive equations with finite differences. In this way, the system of equations can be solved numerically (Anthes 1983). Numerical resolution involves the identification of fixed points (also called nodes) so that each variable is completely

identified by the values assumed at those points. Each grid point identifies a portion of the atmosphere whose characteristics are defined by the value assumed at these points by the variables. There are no limits to the number of nodes to be used, so the only limit is the computing power of the electronic device. For this reason, two main approaches can be taken into account. The first consists of considering the entire atmosphere keeping the distance between two consecutive nodes large, while the second, which involves a better spatial resolution, consists of focusing on a limited area by thickening the grid. There are several weather forecasting models based on the physical parameter values obtained from NWPs. Each of these presents its own features and the differences used the various existing typologies concern:

- the spatial and temporal resolution;
- the used computational techniques;
- the parameterization of physical processes;
- the shape of primitive equations and the numerical methods employed for their solution.

The multiplicity of the models is legitimized by the need to adapt them to the geographical and orographic characteristics of different regions of interest. Of considerable importance are the vertical and horizontal domains. Vertically, the portion of the atmosphere considered is between the troposphere (8 km:12 km) and the stratosphere (15 km:60 km). As above stressed, in relation to the coverage of the horizontal domain, one can distinguish the forecasting models into GMs and LAMs. The former, also known as Global Circulation Models (GCMs) (Phillips 1956; Lewis 1998; Cox 2002; Mechoso and Arakawa 2015), are distinguished by the large scale used that allows to perform predictions over large spaces and for longer times than LAMs. This is one of the reasons why GMs are also applied for the study of the evolution of the globe from a climatological point of view (Chang 1977; Fuà 2006). It is important to note that global models are used to initialize LAMs by providing information at the initial instant that will then be processed on a smaller scale. Among the models with higher performance are Global Forecast System (GFS) and European Center For Medium Range Weather Forecast (ECMWF) (Yang *et al.* 2006; Bechtold *et al.* 2008; Durai and Roy Bhowmik 2014; Zhou *et al.* 2017; Haiden *et al.* 2018). LAMs, also known as regional models, operate on much smaller spatial domains than GM. The main advantage of using them is that they operate with a high grid point density that allows typical spatial resolution values between 1 km and 10 km to be achieved. The increase in resolution gives LAMs the ability to more accurately assess quantities related to mesoscale processes (Davies 2013) and dependent variables such as temperature and pressure at sea level (Mesinger 2001; Castorina *et al.* 2016). In addition, LAMs are able to examine in greater detail the orography of a territory and its influence on atmospheric processes. However, in contrast to the advantages due to the high resolution, it should be noted that LAMs are able to make weather forecasts very accurate over periods of the order of about 48 hours, but this level of detail and precision is not possible in forecasts for longer times (Janjic 2002).

A crucial aspect of any NWP model is the spatial grid on which it is based. This grid is made up of virtual dots (nodes) arranged in a regular way across the globe. The grid allows the atmosphere to be divided into a series of cells, each analyzed to predict future weather conditions. The grid provides a coherent spatial representation of the

atmosphere, it allows the discretization of the physical equations that govern the behavior of the atmosphere and determines the spatial resolution of the model. A finer grid also requires more computational resources, so the choice of spatial resolution is a trade-off between precision and computational cost. An important part of the process of designing numerical weather forecast models is the grid choice that can affect the accuracy and efficiency of forecasts. In fact, each type of grid has advantages and disadvantages and is chosen according to the specific needs of the NWP model (Arakawa and R. 1977; Konor and Randall 2018; Xie 2019). Y. Kurihara (Kurihara 1965) proposed the use of a staggered grid, but today the use of a quasi-uniform grid (used by the GFS model) or the use of a staggered spatial grid (used by the ECMFW model) is widely diffused (Mesinger and Arakawa 1976; Anthes 1983; Miller 1984). After choosing the shape of the grid, it is necessary to select the grid points where to place the prognostic variables (Collins *et al.* 2013). To do this, one can choose to operate through:

- Unstaggered grid in which all variables are placed in the same position within each grid point;
- Staggered grid in which variables are placed at offset locations in the grid point.

As far as the vertical grid is concerned, most models operate in a vertical staggering configuration in which the prognostic variables are placed in the center of the grid, while the vertical velocity is placed at the boundary points between one grid and the adjacent one.

2. WRF

The WRF model (Skamarock *et al.* 2019) is a numerical forecasting system designed to provide high-resolution weather forecasts on a regional scale and plays an essential role in the fields of meteorological research and operational numerical forecasting of atmospheric phenomena (Powers *et al.* 2017). WRF is an open-source model and is a valuable tool for the scientific and meteorological community. These benefits contribute to the continued development of the model and its effectiveness in addressing meteorological challenges around the world. WRF is also highly configurable. In fact, through appropriate files (called namelists) you can choose the settings to be given to the many dynamic and physical parameters present in the code. The software structure of the model was designed with the aim of providing a flexible and scalable platform for weather modelling at a regional scale. One of the key features of the WRF model is its modular structure that offers a number of advantages that contribute to its widespread adoption in the scientific and meteorological community. The core of the model, called WRF Software Framework (WSF), consists of several pre-implemented assimilation and parameterization schemes, to which the pre- and post-processing modules are connected. The dynamics of the WRF model are governed by the following two cores:

- Advanced Research WRF (ARW), developed by NCAR, able to simulate meteorological events of different nature with distinct spatial resolutions. ARW uses a portable code that can work well on different workstations, which is configurable for various applications;
- Non-hydrostatic Mesoscale Model (NMM), developed by NCEP, which can be implemented in hydrostatic and non-hydrostatic modes.

Usually, the former is used for research purposes while the latter for operational numerical forecasting analysis.

The pre-processing phase consists of the preparation of the model input data and is based on the execution of three calculation routines:

- Geogrid: it aims to define the spatial domain of the model and to set up the static data that include orographic and geographical information.
- Ungrib: takes care of the decoding of input data from global GCMs. The input files, which are necessary for initialization and to fix the initial and boundary conditions, must be decoded because they are made available in GRIB format. The GRIB files used by UniMe come from the GFS global model;
- Metgrid: its main objective is to relate the domain set by Geogrid with the data decoded by Ungrib by interpolating them with each other.

The outputs generated by WRF Pre-processing System (WPS) are ready to be processed by WRF. In this context, for the purpose of a correct and truthful analysis, it is necessary to fine-tune the matching between WPS and WRF. Indeed, the nesting conditions, the projection factors and the spatial and temporal domain parameters must remain constant in the two phases. It is recommended, in search applications, to repeat the WPS procedure several times in order to create inputs suitable for the correct execution of the WRF functions. The data coming from the pre-processing phase are processed through special calculation routines. The processing phase consists of the following two basic routines:

- The WRF-REAL software that vertically interpolates the data in the spatial coordinates of the model and generates a file that acts as an input to the WRF routine;
- The WRF software that produces the output data to be analyzed and graphed in the post-processing phase.

Finally, the post-processing phase deals with the extraction of output data and the graphic production to observe the pattern of the different variables.

2.1. WRF model equations. WRF model, through the ARW core, operates by numerically integrating the Navier-Stokes equations into their Eulerian approximation. Euler's approach overlooks viscosity but takes into account compressibility and non-hydrostatic conditions. The equation set integrated by the model can be written as follows.

$$\partial_t U + (\nabla \cdot Vu) - \mu_d \alpha \partial_x p + \frac{\alpha}{\alpha_d} \partial_\eta p \partial_x \phi = F_U \tag{6}$$

$$\partial_t V + (\nabla \cdot Vv) + \mu_d \alpha \partial_y p + \frac{\alpha}{\alpha_d} \partial_\eta p \partial_y \phi = F_V \tag{7}$$

$$\partial_t W + (\nabla \cdot Vw) - g\left[\left(\frac{\alpha}{\alpha_d}\right)\partial_\eta p - \mu_d\right] = F_W \tag{8}$$

$$\partial_t \Theta + (\nabla \cdot V\theta) = F_\Theta \tag{9}$$

$$\partial_t \mu_d + (\nabla \cdot V) = 0 \tag{10}$$

$$\partial_t Q_m + (\nabla \cdot Vq_m) = F_{Qm} \tag{11}$$

where $\alpha_d = \frac{1}{\rho_d}$ is the reverse dry air density. The previous equations also include the humidity effects by adding a term that takes into account the mixing between the various stage of water:

$$\partial_t Q_m + (\nabla \cdot V q_m) = F_{Qm} \tag{12}$$

where

$$Q_m = \mu_d q_m \tag{13}$$

$$q_m = q_v, q_c, q_i, q_r, q_s \tag{14}$$

where q_m considers the mixing ratio of the different hydrometeors included in the calculation. It is also worth noting that the velocity along the vertical axis is expressed by considering the terrain-following η coordinates (Laprise 1992):

$$\eta = \frac{p_h - p_{ht}}{p_{hs} - p_{ht}} \tag{15}$$

where p_h refers to the hydrostatic component, p_{ht} is the pressure on the layer that limits the upper atmosphere, and p_{hs} refers to the surface pressure. Finally, the mass fraction of the air column per area unit is:

$$\mu = p_{hs} - p_{ht} \tag{16}$$

2.2. Initial and boundary conditions. For the WRF model, as well as for all LAMs, it is fundamental to impose boundary and initial conditions derived from a larger scale model (e.g., GFS, ECMWF).Initially, one proceeds by providing the model with static data relating to the geography and orography of the territory. After that, static data are interpolated on the grid. Then one proceeds with the interpolation on the η layers of the boundary and initial conditions, coming from an output of a GCM model. The data includes two-dimensional and three-dimensional field values.

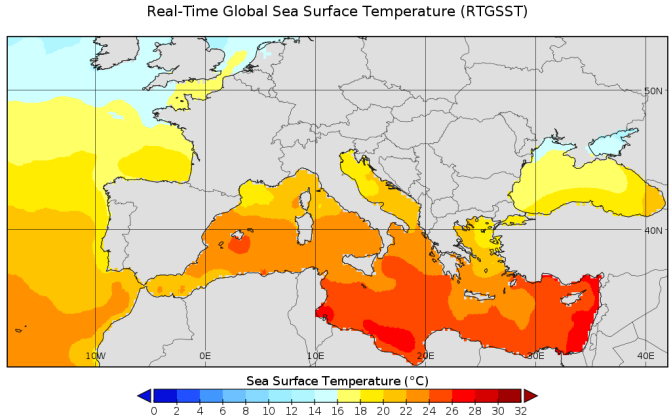

FIGURE 1. Real-Time Global Sea Surface Temperature (RTGSST) of 13 October 2021 with a resolution of 0.083° (available via ftp at: ftp://ftp.ncep.noaa.gov/pub/data/nccf/com/gfs/prod).

The former include, for example, SST (Sea Surface Temperature, see example in Fig. 1), ground pressure and humidity. The latters consist of wind speed, temperature and relative

humidity. Since the η layers are defined in the absence of atmospheric humidity, it is necessary to subtract the wet contribution from the pressure fields to obtain the dry pressure p_{sd} and dry mass μ_d values on all η levels examined. In addition, for boundary conditions, the interpolation takes place from the input of large-scale models.

2.3. Nesting. In order to produce more detailed weather forecasts, the ARW core includes the nesting procedure (S.-C. Wang, Huang, and Li 2006; Jee and Kim 2017). This technique allows one to nest within a main domain, the so-called parent domain, a second finer grid domain with higher resolution, the so-called nested domain (Fig. 2).

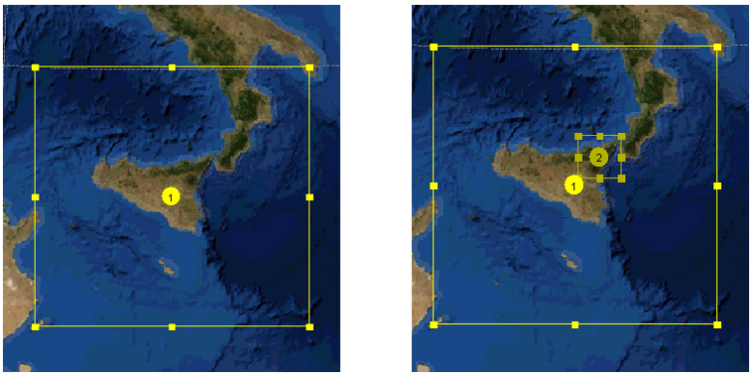

FIGURE 2. Nesting example by means of "Domain Wizard" software.

In this way, the initial and boundary conditions are generated by LAM by means of the outer domain simulation. There are multiple nesting methods in the WRF model. Depending on the type of interaction between the parent domain and the nested domain (W. Wang and Gill 2012; Emmanouil, Vlachogiannis, and Sfetsos 2021), one can distinguish:

- One way nesting: in this case, the transfer of information is unidirectional, from the least resolved grid to the finest one. This configuration can be performed in two different ways. The first is that the outputs generated by the larger grid are used as boundary conditions for the smaller one. The second provides that while the two grids process separately, the nested domain receives the boundary conditions at each time step of the parent domain simultaneously;
- Two-way nesting: in this case the transfer of information occurs bidirectionally from the coarser to the finer grid and vice versa.

Moreover, the variables in the least resolved grid are replaced by those calculated at the same points in the higher resolution grid where the two grid points coincide. This system is extremely advantageous because it allows one to consider, even on a large scale, the processes solved at the smaller scale of the nested domain. To conclude, nesting is an effective technique for obtaining high-resolution weather forecasts in specific areas without having to increase the resolution of the entire domain, which would require more computational resources.

2.4. WRF post-processing. Once the model has generated a weather forecast, the post-processing phase takes place. This step is crucial to convert the model data into useful and understandable information for end users. The WRF-ARW models produces, for each analysis domain, an output called `wrfout_d0*_YYYY-MM-DD_hh:mm:ss`. From this it is possible to extract the data and create weather maps by using graphic processing software. The data extraction procedure must be carried out, as well as for the setting phase, from the command line. On that score the routine `read_wrf_nc` is used to extract the data. To represent data graphically, the most commonly used software are: Ncview, GrADS, NCL, Vapor. These software are distributed free of charge for UNIX-like and Windows operating systems.

2.5. WRF potential applications and extensions. The WRF model, in relation to its good performance in the simulation of regional meteorological conditions, even in the case of extreme weather events, such as heavy rainfall, V-Shaped Storms, flash flood, Mesoscale Convective Systems (MCSs) (Fiori *et al.* 2014; Caccamo *et al.* 2017; Lagasio *et al.* 2019; Castorina *et al.* 2022, 2023), has been one of the most used LAM in the world since its first release around 2000, thus gathering a community of more than 100000 users. One of the main selling points is that it is based on an open-source code, therefore every routine of the model, even the core and the primitive equations, are editable and customizable by the users. In addition, the ARW core provides a significant number of pre-implemented parameterization schemes concerning convection, microphysics, radiative processes, planetary boundary layer and other physical processes, ensuring the versatility of WRF for a wide range of applications in very different contexts (i.e. different geographical locations, very different meteorological conditions).

Furthermore, since the WRF is employed by such a large community of users/developers, it is constantly updating with new options, including parameterization schemes and model extensions. Among the latter, there are:

- WRF-Chem for atmospheric chemistry investigation;
- WRF-Hydro that deals with hydrological modelling;
- WRF-Fire that deals with wildfire modelling.

In this framework, the WRF model along with its extensions represents a powerful tool for studying, analyzing and even predicting various environmental phenomena, from severe weather events to the atmospheric dispersion of pollutants, wildfire and hydrological risk simulation, both in operational and research contexts.

3. WRF-Chem

WRF-Chem is the (WRF) model coupled with Chemistry module. It allows, in addition to the WRF model, to evaluate the processes of emission, transport, sedimentation, dispersion and transformation of all types of pollutants of both natural and anthropic origin (G. A. Grell *et al.* 2005; Rizza *et al.* 2020). WRF-Chem was designed to study the complex interaction between meteorology and atmospheric chemistry. This model, classified as an "online" model, makes it possible to evaluate the evolution of systems both from a meteorological point of view and from that of chemical transformations related to particles present in the atmosphere. One of the greatest advantages of the "online" approach is the possibility of

associating the estimation of air quality with the forecasts of atmospheric phenomena, taking into account the release and transport of aerosols and pollutants (G. Grell and Baklanov 2011). The WRF-Chem model inherited all dynamic core options and parameterizations from the WRF. To conclude, the most important difference between the two models lies in the fact that WRF-Chem is characterized by a chemical section that allows to simulate the presence of tracer gases and atmospheric particulate matter.

4. WRF UniMe

The orographic complexity of the Sicilian territory, characterized by a wide range of mountain profiles, valleys, plains and coasts, is remarkable and significantly influences the weather phenomena. In addition, mountains in Sicily, especially Mt. Etna, Peloritani and Madonie Mounts, are very steep causing the forced uplift of the air masses. In this context, the WRF model represents an important resource for the characterization of a territory such as Sicily. In this section, the characteristics of the hardware and software structures of the WRF model implemented at the Department of Mathematical and Computer Sciences, Physical Sciences and Earth Sciences (MIFT) at Messina University (see scheme in Fig. 3) will be analyzed. Furthermore, the feature of the WRF model working at Messina University (hereafter referred as WRF-UniMe model) will be described. The WRF-UniMe model has been specifically optimized to perform high-resolution numerical weather simulation in a domain covering Sicily and the Mediterranean area. In this context, optimizations and physical parameterizations were deeply investigated in previous work (Caccamo *et al.* 2017; Castorina *et al.* 2018; Castorina, Caccamo, and Magazù 2019; Castorina *et al.* 2021, 2022, 2023).

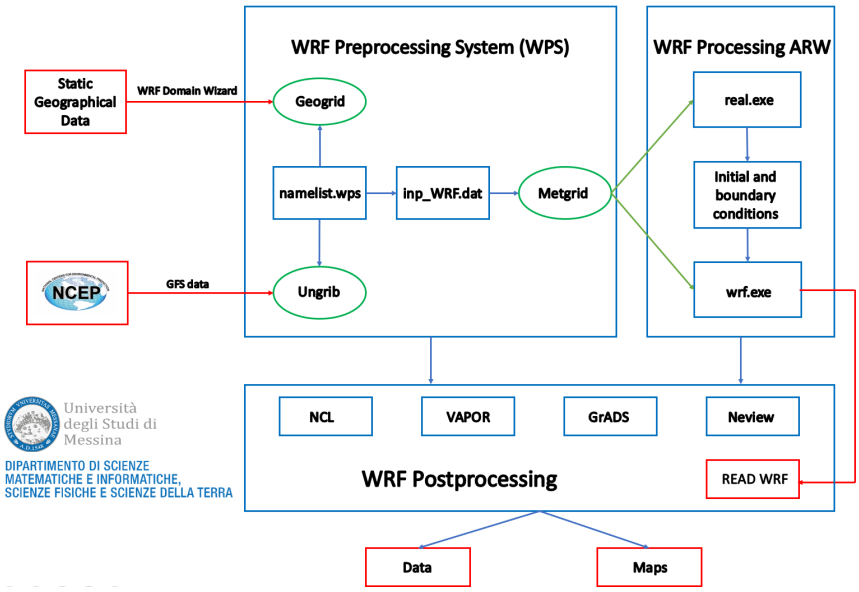

FIGURE 3. Diagram of the WRF UniMe operation processes

4.1. Hardware structure. The hardware structure of (WRF) model implemented at Messina University consists of three servers. All of these are equipped by multicore CPUs from the Intel Xeon family working on Linux environment. In Table 1 the main features of the employed hardware structure (servers) are reported.

TABLE 1. Main features of the employed hardware structure (servers)

Name	Main	Parallelcluster 1	Parallelcluster 2
Frequency (GHz)	2.10	2.20	2.20
n Cores	88	56	56

The server room at the MIFT Department of Messina University hosts the Main and Parallelcluster1 machines, and the third machine (Parallelcluster2) can be found in the Environmental Physics Laboratory within the department. The Main machine works on an operating model and performs two runs per day simulating 72 hours. The first run starts at 18:00 UTC and the second at 00:00 UTC. The Main's analyses are supported by the two parallel machines that aim to perform support runs in severe weather conditions or to perform runs in parallel with input data provided by the ECMWF global model. At the same time, the two parallel machines can be used to carry out analyses by means of WRF-Chem model.

4.2. Software structure. The software architecture of WRF-UniMe's is completely managed from the command line. The Parallelcluster 1 is typically used for post-event simulations. To run simulations, users must have an account (username and password) and know the machine's IP address. Once connected to the server from the UniMe network, one can log in to the machine by running the command `ssh username@IPaddress` from the terminal and entering your password immediately thereafter. Now it is possible to enter the `amministratore` directory (the server paths structure is schematized in Fig. 4). As is well known, the main routines of the pre-processing procedure are sequentially Geogrid, Ungrib and Metgrid. As far as Geogrid is concerned, the WRF model implemented by the University of Messina maintains the domain of forecasting unchanged for the Sicily region in operational configuration. For this reason, one don't need to run Geogrid for every analysis. Therefore, the first step is to download the GRIB files from the GFS global template. There are several GRIB files, such as GFS Forecast and GFS FNL (final gribbed analysis), that are at a resolution of 1 degree (about 100km). For GRIB download, a specific procedure has been implemented. From the `amministratore` directory one can change to `Build_WRF_smpar`. For the grib download one can now run the command `./gribdownload_data.sh` After running the command, one will be asked for the run start date and time. This procedure automatically downloads the gribs that will be ready at the destination. It is now possible to check for GRIB files inside the `GRIBS` folder in the `Build_WRF_smpar` directory. By changing the directory to `2WnestOP`, it is possible to observe the processing of the three routines related to the pre-processing stage and the presence of output files. The folder is self-consistent, allowing analysis using a two-way nesting technique that involves a two-way transfer of information from the coarsest grid

(9 km grid spacing) to the finest grid (3 km grid spacing) and vice versa. In the `2WnestOP` directory one will find the `namelist.input` file where one can change some parameters of the simulation, such as parameterizations. By going back to the `Build_WRF_smpar` directory, the simulation can be run. To do this, you first have to provide the model with the dates to simulate by editing the `inp_WRF.dat` file.

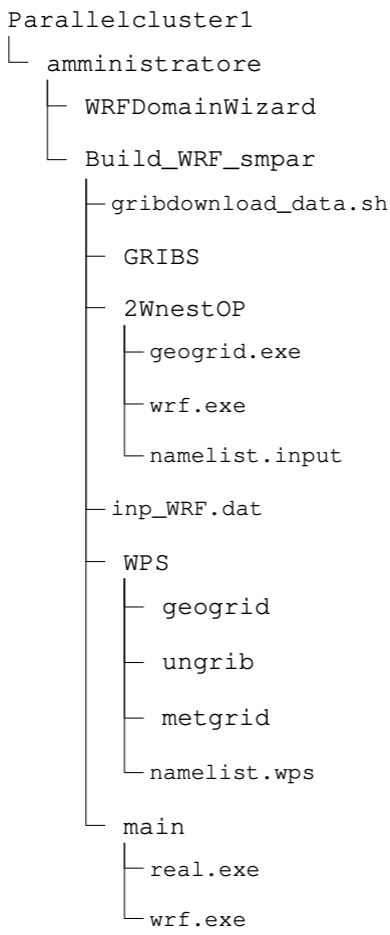

FIGURE 4. Directories organization of the Parallelcluster1 server.

The variables contained within the `inp_WRF.dat` file are listed in the following table:

TABLE 2. List of the variables contained in the `inp_WRF.dat` file

N.	Description
1	Duration in hours of the simulation
2	Year of the run start date
3	Month of the run start date
4	Day of the run start date
5	Run start time (00:00, 06:00, 12:00 or 18:00)
6	Year of the run end date
7	Month of the run end date
8	Day of the run end date
9	Run end time
10	”TEST”
11	”Y” or ”N”
12	Date of the sea temperature

in which, “TEST” is a parameter that can also be modified to choose a parameterization (but this is recommended from the namelist.input file) and “Y” or “N” in case one decide whether or not to provide the model with the sea temperature. To save this file type `esc` and then `wq`. After editing the `inp_WRF.dat` file, one can launch the run of the model using the

```
./lancia_WRF_FNL.sh > mytest_WRF.log &
```

script. Of course, the wording of the `.log` file can be changed, and the analysis process can be controlled by exiting the screen with `CTRL+C` and typing

```
tail -f mytest_WRF.log
```

4.3. Domain choice. Among the many factors that influence the accuracy of WRF predictions, the choice of domain emerges as a crucial step. The size, shape, and location of this domain have a significant impact on the quality of the predictions generated. A careful choice of domain is essential to ensure the correct representation of the specific atmospheric phenomena. Spatial resolution is one of the key aspects to consider. Too large domain could lead to a loss of important local details, while too small domain may not fully capture large-scale atmospheric processes. The topography of the terrain is another element that should not be overlooked, as it can significantly affect the local atmospheric dynamics. The choice of domain is not only about the physical size, but also about the boundary conditions. Initial and boundary conditions are essential for consistent and reliable forecasting. To define the operations to be carried out for the choice of the domain we will refer to the Main but the procedures are the same for all servers. After logging in to the Main you can access the `amministratore` directory than `WRFOPERATIVE` and `WPS` (see scheme in Fig. 5). Within this directory the reference file for the operations we are going to discuss is the `namelist.wps`. In fact, by editing the `namelist.wps` file it is possible to prepare the domain on the area of interest.

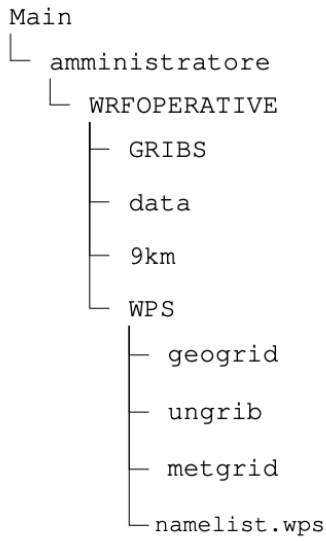

FIGURE 5. Directories organization of the Main server.

During this phase it is necessary to provide the model with the information for the setting of geographic coordinates in decimal values, spatial coordinates for domains, spatial and temporal resolution, ratio for nesting and projection factors. However, setting up the domain correctly can create difficulties such as obtaining precise geographic coordinate values for the analysis domain or declaring the correct number of grid points. To overcome these difficulties, one can use different software such as WRFDomainWizard.

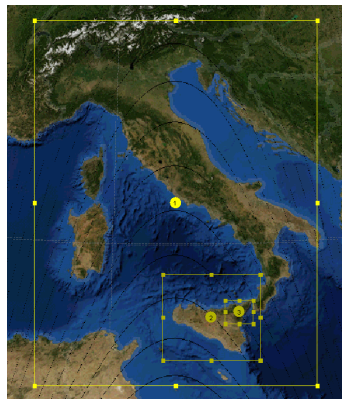

FIGURE 6. Domain choice by means of "Domain Wizard".

This software allows, through a simple interactive graphical interface (Fig. 6), to select the boundaries of the primary spatial domain and any nesting domains on a virtual world

map. In addition, WRFDomainWizard is able to provide numeric values in the same format as those required by the WPS setting file. The WRF model implemented by UniMe uses the ARW dynamic core, which operates by means of the "Lambert Conformal,, projection. The first thing to specify within WRFDomainWizard is precisely the projection used by the dynamic core of the model along with all the projection options (True Lat 1 and True Lat 2). Next, one needs to provide grid options in terms of: horizontal dimension X, horizontal dimension Y, grid points distance (km) and geographic data resolution. At the end of this step, the software is able to provide the numerical values to be entered into the `namelist.wps` file. The domain choice in the WRF model is a strategic component that requires a careful approach based on the specific characteristics of the interest area. Only through careful domain selection is it possible to maximize the reliability of weather forecasts and contribute significantly to the understanding and management of atmospheric phenomena.

4.4. Data Transposing Protocol. A crucial step of our in-depth analysis involves transposing the data in order to create an analysis report. This process is critical to presenting our findings in a clear and accessible format, facilitating effective communication. For the data transposing procedure we will refer to the steps to be followed on the Parallelcluster1 but these are the same on all servers. After logging in to the Parallelcluster1, from the `amministratore` directory one need to go to the `READ_WRF` directory and then `DRPC`. This folder contains the scripts implemented for extracting data that are renamed based on run start time (00:00 or 18:00). If, for example, one wants to extract the simulated data in the run started at 00:00, we run the corresponding script with the following command:

```
./analisi00.sh
```

At this point, one will be asked for the year, month, and day of the run start date. This starts the data extraction procedure that ends with the creation of files, a different one for each surveillance zone, listing data on both maximum and average rainfall accumulations. In addition, minimum temperature, maximum temperatures and maximum wind gusts are arranged in three different files in which the values extracted are distinguished based on surveillance zone. These files will be stored in a sub-folder of the `DATI_3ORE_RUN00` (see location in Fig. 4) one renamed based on the date initially provided. After having acquired the data, it is immediate their transposition for the realization of the report.

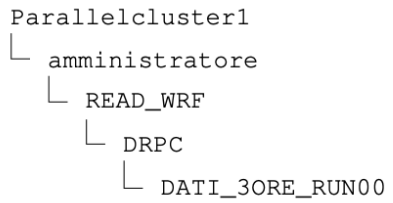

FIGURE 7. Diagram of the WRF-Chem UniMe operation processes

5. WRF-Chem UniMe

WRF-Chem model is employed for forecasting volcanic ash and desert dust diffusion over Sicily and central Mediterranean. For this purpose, in this section the main steps of management and use of the model will be analyzed. The software management of the WRF-Chem model implemented by UniMe is not so different from the one previously analyzed for the WRF model (scheme in Fig. 8). In the following, we will refer to the Parallelcluster1 server which is usually employed for WRF-Chem simulations.

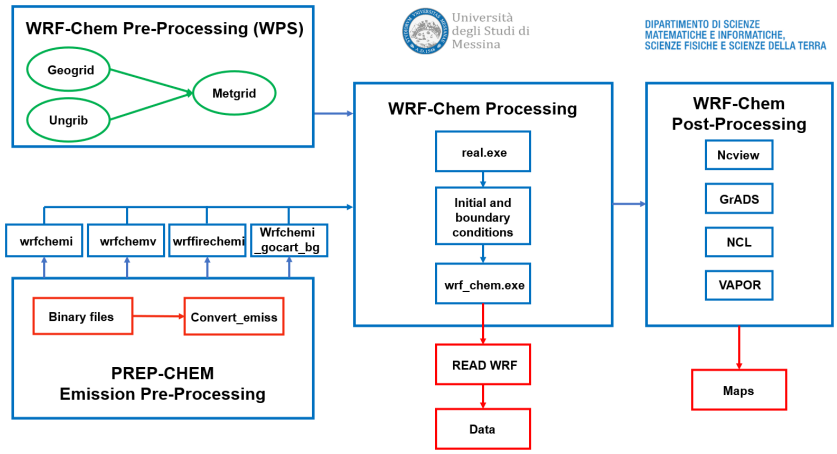

FIGURE 8. Diagram of the WRF-Chem UniMe operation processes

After logging in to Parallelcluster1 (structure scheme in Fig. 7), one can enter the `amministratore` directory. One can now change to `Build_WRF_Chem_gfortran` directory and download the .grib files by running the `gribdownload_data.sh` command. From the `RUN_3km` directory it is possible to access the `namelist.input` file, which has a similar structure to the one seen for the WRF model, but the difference lies in the `chem` section. From the `Build_WRF_Chem_gfortran` directory one can check for grib files inside the `GRIBS` folder. To run the simulation directly from this directory, you need to provide the model with the dates to be simulated by editing the `inp_WRF_Chem.dat` file. The variables to be specified within this file are, in addition to those seen above for the `inp_WRF_Chem.dat` file, the eruption start time and start minute. One now needs to change the directory to `Build_WRF_Chem_gfortran` and edit the `etna_3km.sh` script to provide the template with the correct dates for PREP-CHEM purposes. PREP-CHEM is a preprocessor that simulates volcanic emission or other phenomena. The accuracy of the simulation is strongly influenced by the information provided to the model during the Prep Chem phase regarding the eruptive characteristics of the volcano, for example: the height of the plume, eruption time, geographical coordinates, rate of erupted mass, grain size. To provide the geographical coordinates of the volcano it will be necessary to change directory to the `Build_WRF_Chem` one, than `ANALISI` and than one have to modify the `prep_chem_source.inp` script by inserting the volcano index (e.g., Etna index is 15).

By editing the first line of the file `Etna.dat` it will be possible to provide information on the maximum height of the eruptive column (m), the event duration (s), total mass of ash erupted (kg), total mass of SO_2 erupted (kg). In the second row one will need to enter the breakdown of the grain size.

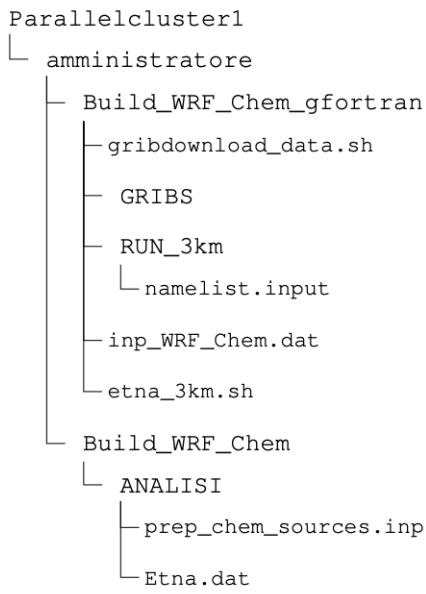

FIGURE 9. Diagram of the WRF-Chem UniMe operation processes

The so called Mastin's scheme (Mastin *et al.* 2009) provides a classification of volcanoes into eleven categories on the basis of registered eruptive features. More in detail, the Mastin's classification scheme associates a given dimensional spectrum to each of the eleven categories of volcanoes on the basis of the volcanic ash effective diameter, through a histogram containing 10 bins, each of them corresponding to a specific diameter range. The first bin is used for volcanic particles with a diameter value ranging from 1mm to 2 mm while the last one encompasses ashes with a diameter value $< 3.9\mu m$. Conventionally, the particle size, for each category, is characterized by the percentage of mass fraction of the particles that fall into the different bins. The Stuefer's empirical formula (Stuefer *et al.* 2012) is usually employed to evaluate the mass of ash ejected from the volcanic crater:

$$m = \rho d(0.0005h)^{4.1494} \tag{17}$$

where h is the height of the plume, d is the duration of the eruptive process, and ρ is the density usually assumed between 2500 Kg/m^3 and 2600 Kg/m^3. Based on this formula, it is possible to determine the rate of the erupted mass as the m/d ratio. As far as the mass of erupted SO_2 is concerned, it is possible to consider, as an example, the data provided

by the "Multi-Satellite Volcanic Sulfur Dioxide L4 Long-Term Global Database of NASA" database created on the basis of multi-satellite interpolations performed by NASA.

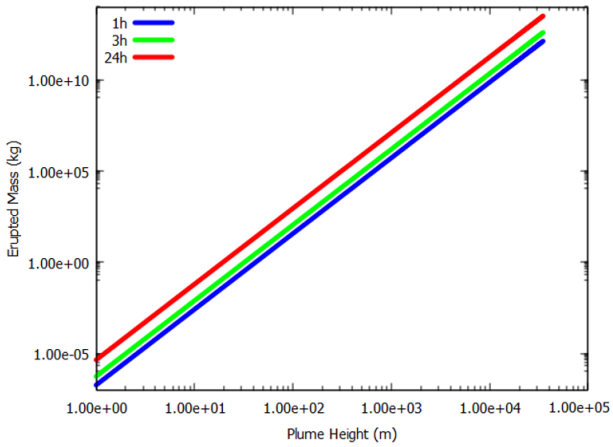

FIGURE 10. Erupted mass [kg] vs plume height [m] according to the linearized Stuefer formula. In the graph, both axes are on a logarithmic scale, and the three curves refer to three different eruption durations, namely 1 hour (blue), 3 hours (green), and 24 hours (red).

At the end of these operations, one can launch the model through the

```
./lancia_WRF_Chem_FNL.sh > mytest_WRF_Chem.log &
```

Furthermore, Dynamic Light Scattering (DLS) measurements using a Zetasizer ULTRA - Blue Label instrument have recently been conducted on solutions containing extremely fine volcanic ash particles. This technique employs the principle of Brownian motion to measure the size distribution of particles in a suspension. Zetasizer ULTRA, specifically the Blue Label model, is equipped with advanced features that enhance the accuracy and resolution of particle size measurements; its capabilities include a high sensitivity to detect even the smallest particles and a wide measurement range, making it ideal for studying diverse particulate sizes. The utilization of the Zetasizer ULTRA allowed for precise determination of the mean size of the volcanic ash particles. Additionally, it provided a comprehensive characterization of the dimensional distribution of the ash. This analysis is crucial for several reasons; firstly, understanding the particle size distribution helps in assessing the potential for atmospheric dispersion and sedimentation behaviors of the ash, which are critical factors in predicting the impact on air quality and health; moreover, such detailed characterization of volcanic ash particles enhances the refinement of atmospheric dispersion models, such as the Weather Research and Forecasting model coupled with Chemistry (WRF-Chem). By integrating more accurate particle size data into the model, predictions of ash dispersion can be significantly improved. This includes better forecasting of the spread of ash clouds over large distances from the volcano. The initial findings have prompted plans to expand this analysis to include different volcanic eruption events. By comparing the

particle size distributions from various Etna's eruptions, we aim to develop a more robust understanding of the relationships between eruption dynamics, ash particle characteristics, and their subsequent behavior in the atmosphere. This comparative approach will not only refine existing models but also aid in the development of targeted mitigation strategies to manage the effects of volcanic ash on both local and global scales.

6. Application to real case studies

In order to assess the predictive performances of both WRF and WRF-Chem models, two events were selected as case studies. The first one concerns a severe weather event that occurred in Sicily on 13 and 14 October 2021, while the second one is focused on the simulation of the volcanic ash dispersion from the paroxysmal activity of Mt. Etna.

6.1. Rainfall prediction on 13-14 October 2021. During the days of 13 and 14 October Sicily was affected by a low-pressure system causing intense rainfall. In particular, huge rainfall accumulations were recorded on the northern sector of the Island between the afternoon of 13 and early 14 October 2021, while the southeastern one was affected by intense precipitation in the morning of 14 October 2021. The observed phenomena also provoked floods, troubles to the road network and localised landslides and collapses. In this context, several simulations were carried out by using the WRF-UniMe model which were aimed at forecasting the event. Among these, the simulation started at 00:00 UTC of 13 October 2021, running in operational forecast mode, has been selected to be analyzed. Specifically, the predicted 24h rainfall maps of 13 and 14 October were compared with the maps of 24h rainfall accumulations recorded by the weather stations belonging to the DRPC (Dipartimento Regionale della Protezione Civile) network. The comparison is shown below.

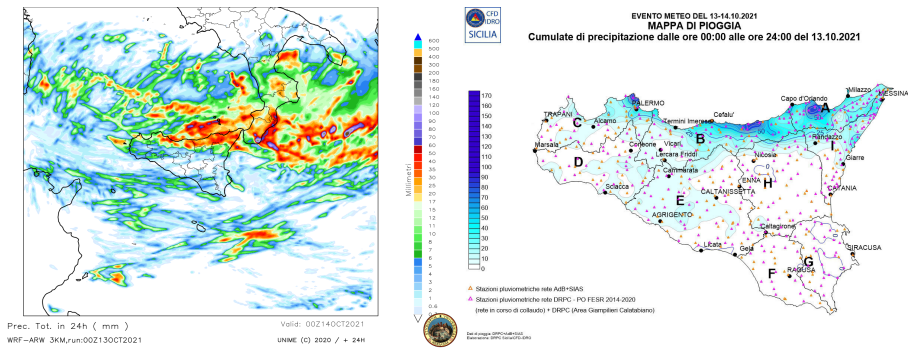

FIGURE 11. Comparison between 24h rainfall map obtained from the WRF simulation (left) and observed rainfall recorded by the DRPC weather stations network (right) from 00:00 UTC of 13 and 00:00 UTC of 14 October 2021.

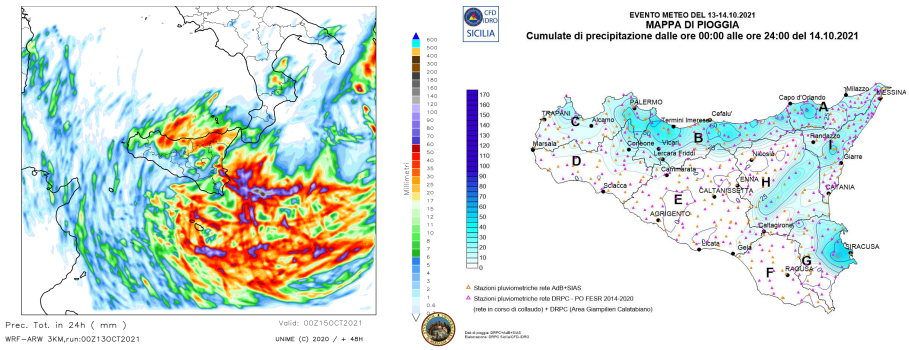

FIGURE 12. Comparison between 24h rainfall map obtained from the WRF simulation (left) and observed rainfall recorded by the DRPC weather stations network (right) from 00:00 UTC of 14 and 00:00 UTC of 15 October 2021.

Moreover, the comparison between simulated and observed 48h rainfall maps is proposed.

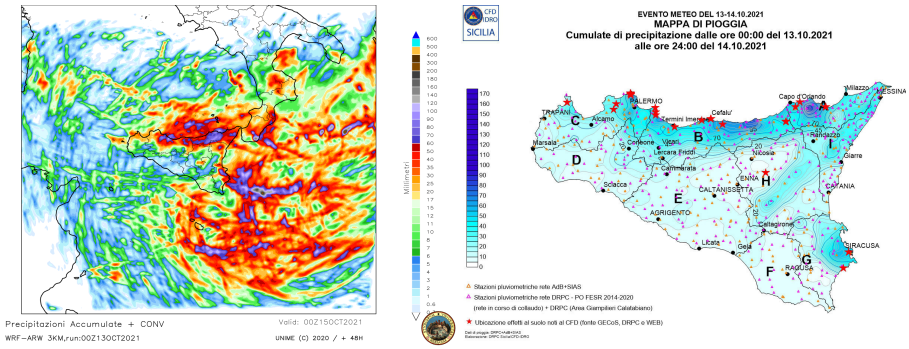

FIGURE 13. Comparison between 48h rainfall map obtained from the WRF simulation (left) and observed rainfall recorded by the DRPC weather stations network (right) from 00:00 UTC of 13 and 00:00 UTC of 15 October 2021.

The comparisons show a good agreement between the spatial distribution of the rainfall accumulations predicted by the WRF-UniMe model and the rainfall observed by the DRPC weather stations network. Even the value of rainfall accumulations is in line with the observations, albeit slightly underestimated.

6.2. Ash dispersion simulation at Mt. Etna volcano (10 February 2022). During the evening of 10 February 2022 a paroxysm occurred at Mt. Etna. Starting from the afternoon, an intense "Strombolian" activity was recorded at the South East Crater (SEC); around 20:40 UTC the activity passed into lava fountain, causing the formation of an ash-rich column of 10000 meters at the top. In this framework, with the aim to test the performance of the WRF-Chem model in simulating the atmospheric dispersion of the volcanic ash emitted by Mt. Etna, a simulation was carried out. The simulated ash maps are shown in

Fig. 14, jointly with the observed map retrieved from MGS SEVIRI satellite[1] (Aminou, Jacquet, and Pasternak 1997; Aminou *et al.* 1999; Stengel *et al.* 2014).

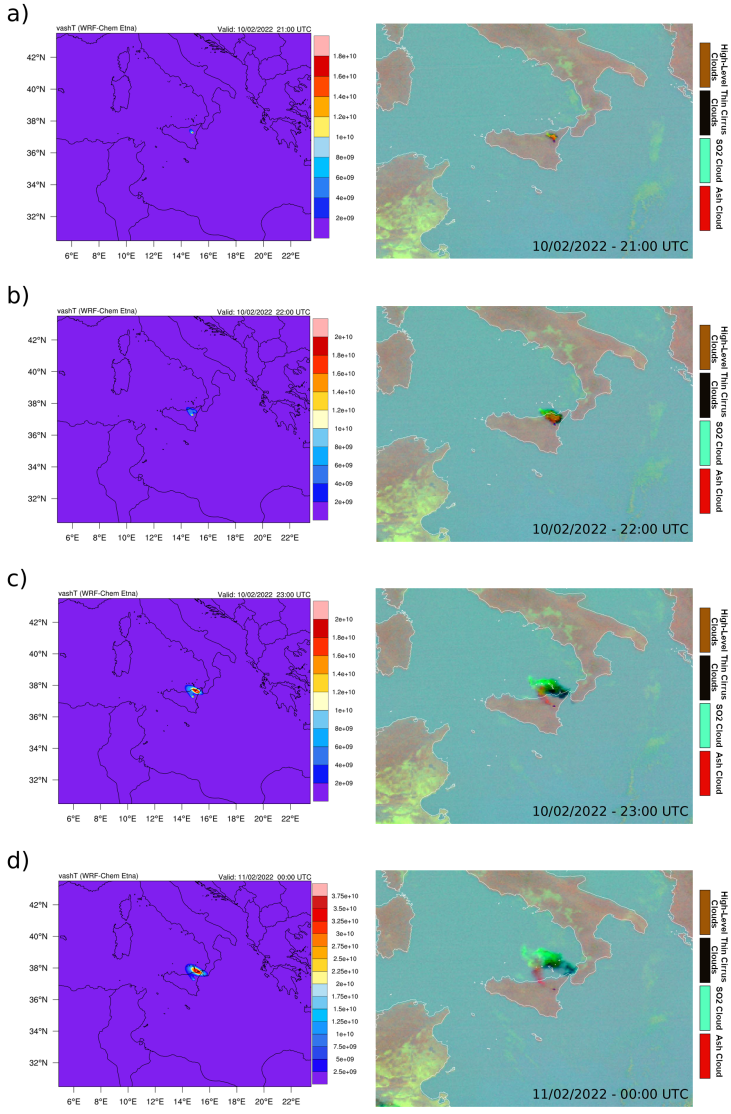

FIGURE 14. Comparison between hourly columnar ash [g m^{-2}] maps simulated by the WRF-Chem (left) and the ash RGB images detected by the SEVIRI satellite (right) at 21:00 (panel a), 22:00 (panel b), 23:00 (panel c) UTC of 10 February 2022 and 00:00 UTC (panel d) of 11 February 2022.

[1]URL: https://www.eumetsat.int/seviri

The WRF-Chem simulation predicted a plume dispersion towards the north-western quadrants, according to atmospheric conditions. The comparisons highlight the good agreement between the simulated ash spatial pattern and that observed by the satellite.

7. Conclusions

The present work deals with the role of Numerical Weather Prediction (NWP) models in understanding and in forecasting atmospheric conditions. On that score, the primitive equations on which most of the developed models are based have been considered, with specific reference to the WRF model and to its calculation routines. The WRF model constitutes a fundamental resource in the field of numerical weather forecasting due to its flexibility and its adaptability. Thanks to its advanced design and its effective algorithms, the WRF model has shown a great capability to produce accurate and detailed weather forecasts, especially on a local scale. For these reasons, the WRF model is diffusely employed by the University of Messina for the study of meteorological conditions concerning the Sicily region. The Mediterranean region, and particularly Sicily, is characterized by complex geophysical and orographic features that are well managed by the WRF model. Furthermore, due to the presence of active volcanoes in Sicily, the coupling of the WRF model with the Chem extension is also used for forecasting of volcanic ash diffusion. In this framework, the present contribution firstly focuses on the optimization processes employed on the standard WRF and WRF-Chem models that have been properly customized to Sicily. Furthermore, a detailed description of the hardware and software structures and the employed management procedures are dealt with. Finally, in order to show the predictive properties of the two implemented models, two case studies are presented. As far as the WRF case study is concerned, a meteorological event that affected Sicily, and particularly the eastern part of the region, on 13rd and 14th October 2021, has been investigated. This event is particularly important for testing the capabilities of the model due to the fact that it exhibited a highly localized behavior, both in terms of time and space. The comparison between the data extracted from the simulations performed by the customized model in operational forecast mode and the rainfall observed by the DRPC network of weather stations highlights the excellent predictive capabilities of the model both in northeastern and southeastern Sicily. Moreover, the results of a case study concerning the employment of the WRF-Chem model to an eruptive event of the Etna volcano are presented. Even in this case, the model shows very good performance, as the simulated ash dispersion pattern is in agreement with satellite data. To conclude, the results obtained from the performed simulations suggest that WRF and WRF-Chem UniMe, suitably adapted for the specific geographic area analyzed, represent a reliable tool for accurate forecasts, including localized severe meteorological phenomena and volcanic ash dispersion.

Future developments will include i) the integration between WRF model and data retrieved from satellite systems by using data assimilation techniques, ii) the execution of simultaneous simulations considering different initialization conditions (grib files, parameterizations) in operational forecast mode, while from a computational point of view iii) the system may be enhanced by implementing the GPU computing.

Acknowledgements

This work is to be framed within the "ESCAPE - Economic and Social Consequences of Altered Planet Environment" Project, CUP J43C24000400006,in the frame of PE00000018 GRINS – Growing Resilient, INclusive and Sustainable BAC PNRR project M4-C2-1.3 - NextGeneration EU – D.R. 4149 del 31/10/2023.

References

Aminou, D. M. A., Jacquet, B., and Pasternak, F. (1997). "Characteristics of the Meteosat Second Generation (MSG) radiometer/imager: SEVIRI". In: *Sensors, Systems, and Next-Generation Satellites*. Ed. by H. Fujisada. SPIE. DOI: 10.1117/12.298084.

Aminou, D. M. A., Ottenbacher, A., Jacquet, B., and Kassighian, A. (1999). "Meteosat second generation: on-ground calibration, characterization, and sensitivity analysis of the SEVIRI imaging radiometer". In: *Earth Observing Systems IV*. Ed. by W. L. Barnes. SPIE. DOI: 10.1117/12.363538.

Anthes, R. (1983). "Regional Models of the Atmosphere in Middle Latitudes". *Monthly Weather Review* **111**, 1306–1335. DOI: 10.1175/1520-0493(1983)111<1306:RMOTAI>2.0.CO;2.

Arakawa, A. and R., L. V. (1977). "Computational Design of the Basic Dynamical Processes of the UCLA General Circulation Model". In: *Methods in Computational Physics: Advances in Research and Applications*. Ed. by J. Chang. Vol. 17. Elsevier, pp. 173–265. DOI: 10.1016/b978-0-12-460817-7.50009-4.

Bechtold, P., Köhler, M., Jung, T., Doblas-Reyes, F., Leutbecher, M., Rodwell, M. J., Vitart, F., and Balsamo, G. (2008). "Advances in simulating atmospheric variability with the ECMWF model: From synoptic to decadal time-scales". *Quarterly Journal of the Royal Meteorological Society* **134**(634), 1337–1351. DOI: 10.1002/qj.289.

Caccamo, M. T., Castorina, G., Colombo, F., Insinga, V., Maiorana, E., and Magazù, S. (2017). "Weather forecast performances for complex orographic areas: Impact of different grid resolutions and of geographic data on heavy rainfall event simulations in Sicily". *Atmospheric Research* **198**, 22–33. DOI: 10.1016/j.atmosres.2017.07.028.

Castorina, G., Caccamo, M. T., Colombo, F., Insinga, V., Maiorana, E., and Magazù, S. (2016). "Sviluppo e ottimizzazione di un modello fisico–matematico ad area limitata e ad alta risoluzione per la previsione di dati meteorologici". In: *Atti della Conferenza ASITA 2016*. Cagliari, Italia.

Castorina, G., Caccamo, M. T., Colombo, F., and Magazù, S. (2021). "The Role of Physical Parameterizations on the Numerical Weather Prediction: Impact of Different Cumulus Schemes on Weather Forecasting on Complex Orographic Areas". *Atmosphere* **12**(5), 616. DOI: 10.3390/atmos12050616.

Castorina, G., Caccamo, M. T., Insinga, V., Magazù, S., Munaò, G., Ortega, C., Semprebello, A., and Rizza, U. (2022). "Impact of the Different Grid Resolutions of the WRF Model for the Forecasting of the Flood Event of 15 July 2020 in Palermo (Italy)". *Atmosphere* **13**(10), 1717. DOI: 10.3390/atmos13101717.

Castorina, G., Semprebello, A., Insinga, V., Italiano, F., Caccamo, M. T., Magazù, S., Morichetti, M., and Rizza, U. (2023). "Performance of the WRF Model for the Forecasting of the V-Shaped Storm Recorded on 11–12 November 2019 in the Eastern Sicily". *Atmosphere* **14**(2), 390. DOI: 10.3390/atmos14020390.

Castorina, G., Caccamo, M. T., and Magazù, S. (2019). "Study of convective motions and analysis of the impact of physical parametrization on the WRF-ARW forecast model". *Atti della Accademia Peloritana dei Pericolanti. Classe di Scienze Fisiche, Matematiche e Naturali* **97**(S2), A19 [16 pages]. DOI: 10.1478/AAPP.97S2A19.

Castorina, G., Caccamo, M. T., Magazù, S., and Restuccia, L. (2018). "Multiscale mathematical and physical model for the study of nucleation processes in meteorology". *Atti della Accademia Peloritana dei Pericolanti. Classe di Scienze Fisiche, Matematiche e Naturali* **96**(S3), A6 [12 pages]. DOI: 10.1478/AAPP.96S3A6.

Chang, J. (1977). *General circulation models of the atmosphere*. New York: Academic Press.

Collins, S. N., Robert, S., Ray, P., Chen, K., Lassman, A., and Brownlee, J. (2013). "Grids in Numerical Weather and Climate Models". In: *Climate Change and Regional/Local Responses*. Ed. by Y. Zhang and P. Ray. Rijeka: IntechOpen. Chap. 4. DOI: 10.5772/55922.

Cox, J. D. (2002). *Storm Watchers: The Turbulent History of Weather Prediction from Franklin's Kite to El Niño*. New York: John Wiley & Sons.

Davies, T. (2013). "Lateral boundary conditions for limited area models". *Quarterly Journal of the Royal Meteorological Society* **140**(678), 185–196. DOI: 10.1002/qj.2127.

Durai, V. and Roy Bhowmik, S. (2014). "Prediction of Indian summer monsoon in short to medium range time scale with high resolution global forecast system (GFS) T574 and T382". *Climate Dynamics* **42**, 1527–1551. DOI: 10.1007/s00382-013-1895-5.

Emmanouil, G., Vlachogiannis, D., and Sfetsos, A. (2021). "Exploring the ability of the WRF-ARW atmospheric model to simulate different meteorological conditions in Greece". *Atmospheric Research* **247**, 105226. DOI: 10.1016/j.atmosres.2020.105226.

Fiori, E., Comellas, A., Molini, L., Rebora, N., Siccardi, F., Gochis, D., Tanelli, S., and Parodi, A. (2014). "Analysis and hindcast simulations of an extreme rainfall event in the Mediterranean area: The Genoa 2011 case". *Atmospheric Research* **138**, 13–29. DOI: 10.1016/j.atmosres.2013.10.007.

Fuà, D. (2006). "La previsione meteorologica, nascita ed evoluzione dei modelli". *emmeciquadro* **26**, 7–20. URL: https://web.archive.org/web/20090709152502/http://g24ux.phys.uniroma1.it/pubblicazioni/MC2_2006_FUA.pdf.

Grell, G. A., Peckham, S. E., Schmitz, R., McKeen, S. A., Frost, G., Skamarock, W. C., and Eder, B. (2005). "Fully coupled online chemistry within the WRF model". *Atmospheric Environment* **39**(37), 6957–6975. DOI: 10.1016/j.atmosenv.2005.04.027.

Grell, G. and Baklanov, A. (2011). "Integrated modeling for forecasting weather and air quality: A call for fully coupled approaches". *Atmospheric Environment* **45**(38). Modeling of Air Quality Impacts, Forecasting and Interactions with Climate., 6845–6851. DOI: 10.1016/j.atmosenv.2011.01.017.

Haiden, T., Janousek, M., Vitart, F., Bouallègue, Z. B., Ferranti, L., Prates, F., and Richardson, D. (2018). *Evaluation of ECMWF forecasts, including the 2018 upgrade*. Technical Memorandum 837. Reading, UK: European Centre for Medium-Range Weather Forecasts. URL: https://www.ecmwf.int/en/elibrary/18765-evaluation-ecmwf-forecasts-including-2018-upgrade.

Holton, J. R. (2004). *An Introduction to Dynamic Meteorology*. 4th ed. Vol. 88. International Geophysics. Burlington, MA: Academic Press.

Janjic, Z. (2002). *Nonsingular Implementation of the Mellor–Yamada Level 2.5 Scheme in the NCEP Meso Model*. Office Note 436. Camp Springs, MD: National Centers for Environmental Prediction (NCEP).

Jee, J.-B. and Kim, S. (2017). "Sensitivity Study on High-Resolution WRF Precipitation Forecast for a Heavy Rainfall Event". *Atmosphere* **8**(6), 96. DOI: 10.3390/atmos8060096.

John M. Wallace, P. V. H. (2006). *Atmospheric Science*. Elsevier LTD, Oxford. 504 pages. URL: https://www.ebook.de/de/product/4444872/john_m_wallace_peter_v_hobbs_atmospheric_science.html.

Konor, C. S. and Randall, D. A. (2018). "Impacts of the horizontal and vertical grids on the numerical solutions of the dynamical equations Part 1: Nonhydrostatic inertia gravity modes". *Geoscientific Model Development* **11**(5), 1753–1784. DOI: 10.5194/gmd-11-1753-2018.

Kurihara, Y. (1965). "Numerical Integration of the Primitive Equations on a Spherical Grid". *Monthly Weather Review* **93**(7), 399–415. DOI: 10.1175/1520-0493(1965)093<0399:niotpe>2.3.co;2.

Lagasio, M., Silvestro, F., Campo, L., and Parodi, A. (2019). "Predictive Capability of a High-Resolution Hydrometeorological Forecasting Framework Coupling WRF Cycling 3DVAR and Continuum". *Journal of Hydrometeorology* **20**(7), 1307–1337. DOI: 10.1175/JHM-D-18-0219.1.

Laprise, R. (1992). "The Euler Equations of Motion with Hydrostatic Pressure as an Independent Variable". *Monthly Weather Review* **120**(1), 197–207. DOI: 10.1175/1520-0493(1992)120<0197:teeomw>2.0.co;2.

Lewis, J. M. (1998). "Clarifying the Dynamics of the General Circulation: Phillips 1956 Experiment". *Bulletin of the American Meteorological Society* **79**(1), 39–60. DOI: 10.1175/1520-0477(1998)079<0039:ctdotg>2.0.co;2.

Lynch, P. (2007). "Foreword". In: *Weather Prediction by Numerical Process*. Dublin: UCD.

Mastin, L. G., Guffanti, M., Servranckx, R., Webley, P., Barsotti, S., Dean, K., Durant, A., Ewert, J. W., Neri, A., Rose, W. I., Schneider, D., Siebert, L., Stunder, B., Swanson, G., Tupper, A., Volentik, A., and Waythomas, C. F. (2009). "A multidisciplinary effort to assign realistic source parameters to models of volcanic ash-cloud transport and dispersion during eruptions". *Journal of Volcanology and Geothermal Research*. DOI: 10.1016/j.jvolgeores.2009.01.008.

Mechoso, C. R. and Arakawa, A. (2015). "Numerical Models | General Circulation Models". In: *Encyclopedia of Atmospheric Sciences*. Ed. by G. R. North, J. Pyle, and F. Zhang. 2nd ed. Oxford: Academic Press, pp. 153–160. DOI: 10.1016/b978-0-12-382225-3.00157-2.

Mesinger, F. (2001). *Limited Area Modeling: Beginnings, state of the art, outlook*. Ruksaldruck, Berlin.

Mesinger, F. and Arakawa, A. (1976). *Numerical Methods Used in Atmospheric Models*. Vol. 1. GARP Publication Series 17. WMO – ICSU Joint Organizing Committee. Geneva.

Miller, M. J. (1984). "Numerical prediction and dynamic meteorology (2nd Edition). G. J. Haltiner and R. T. Williams. J. Wiley and Sons Ltd. 1983. xiii pp. 477," *Quarterly Journal of the Royal Meteorological Society* **110**(463), 280–280. DOI: 10.1002/qj.49711046321.

Phillips, N. A. (1956). "The general circulation of the atmosphere: A numerical experiment". *Quarterly Journal of the Royal Meteorological Society* **82**(352), 123–164. DOI: 10.1002/qj.49708235202.

Pielke Sr, R. A. (2013). *Mesoscale Meteorological Modeling, Volume 98*. Academic Pr Inc. 760 pages. URL: https://www.ebook.de/de/product/20679239/roger_a_pielke_sr_mesoscale_meteorological_modeling_volume_98.html.

Powers, J. G., Klemp, J. B., Skamarock, W. C., Davis, C. A., Dudhia, J., Gill, D. O., Coen, J. L., Gochis, D. J., Ahmadov, R., Peckham, S. E., Grell, G. A., Michalakes, J., Trahan, S., Benjamin, S. G., Alexander, C. R., Dimego, G. J., Wang, W., Schwartz, C. S., Romine, G. S., Liu, Z., Snyder, C., Chen, F., Barlage, M. J., Yu, W., and Duda, M. G. (2017). "The Weather Research and Forecasting Model: Overview, System Efforts, and Future Directions". *Bulletin of the American Meteorological Society* **98**(8), 1717–1737. DOI: 10.1175/bams-d-15-00308.1.

Rizza, U., Brega, E., Caccamo, M. T., Castorina, G., Morichetti, M., Munaò, G., Passerini, G., and Magazù, S. (2020). "Analysis of the ETNA 2015 Eruption Using WRF-Chem Model and Satellite Observations". *Atmosphere* **11**(11), 1168. DOI: 10.3390/atmos11111168.

Scotton, R., Mercalli, L., Castellano, C., and Berro, D. C. (2003). "Introduzione ai modelli numerici diprevisione meteorologica (NWP)". *Nimbus 29-30, Meteorologia*.

Skamarock, W. C., Klemp, J. B., Dudhia, J., Gill, D. O., Liu, Z., Berner, J., Wang, W., Powers, J. G., Duda, M. G., Barker, D. M., and Huang, X.-Y. (2019). *A Description of the Advanced Research WRF Model Version 4.1*. NCAR Technical Note NCAR/TN-556+STR. Boulder, CO: National Center for Atmospheric Research. DOI: 10.5065/1dfh-6p97.

Stengel, M., Kniffka, A., Meirink, J. F., Lockhoff, M., Tan, J., and Hollmann, R. (2014). "CLAAS: the CM SAF cloud property data set using SEVIRI". *Atmospheric Chemistry and Physics* **14**(8), 4297–4311. DOI: 10.5194/acp-14-4297-2014.

Stuefer, M., Freitas, S., Grell, G., Webley, P., Peckham, S., and McKeen, S. (2012). "Inclusion of Ash and SO2 emissions from volcanic eruptions in WRF-CHEM: development and some applications". *Geoscientific Model Development Discussions* **5**, 2571–2597. DOI: 10.5194/gmdd-5-2571-2012.

Wang, S.-C., Huang, S.-X., and Li, Y. (2006). "Sensitive Numerical Simulation and Analysis of Rainstorm Using Nested WRF Model". *Journal of Hydrodynamics* **18**(5), 578–586. DOI: 10.1016/s1001-6058(06)60138-8.

Wang, W. and Gill, D. (2012). *WRF Nesting*. WRF Tutorial, University of São Paulo, Brazil. URL: https://www.mce2.org/11_aug_5_nest_set_up_and_run%20%28Dave%20Gill%29.pdf.

Xie, Y. (2019). "Generalized Z-Grid Model for Numerical Weather Prediction". *Atmosphere* **10**(4), 179. DOI: 10.3390/atmos10040179.

Yang, F., Pan, H.-L., Krueger, S. K., Moorthi, S., and Lord, S. J. (2006). "Evaluation of the NCEP Global Forecast System at the ARM SGP Site". *Monthly Weather Review* **134**(12), 3668–3690. DOI: 10.1175/MWR3264.1.

Zhou, X., Zhu, Y., Hou, D., Luo, Y., Peng, J., and Wobus, R. (2017). "Performance of the new NCEP Global Ensemble Forecast System in a parallel experiment". *Weather and Forecasting* **32**(5), 1989–2004. DOI: 10.1175/WAF-D-17-0023.1.

---

[a] Università degli Studi di Messina,
Dipartimento di Scienze Matematiche e Informatiche, Scienze Fisiche e Scienze della Terra,
Viale F. Stagno d'Alcontres, 31, 98166 Messina, Italy

[b] Istituto Nazionale di Geofisica e Vulcanologia (INGV),
Sezione di Palermo, Sede Operativa di Milazzo,
Via dei Mille, 98057 Milazzo, Italy

[*] To whom correspondence should be addressed | email: smagazu@unime.it

Communicated 27 November 2023; manuscript received 10 June 2024; published online 10 May 2025